

**IMPROVEMENT OF THE PROCESSING OF INITIAL CONDITIONS OF
PARTICLES UNDERGOING DEP EFFECTS IN HOMOGENOUS
SUSPENSION USING MATLAB**

NOOR HIDAYAH BT. AMIR HASSAN

**INSTITUTE OF GRADUATE STUDIES
UNIVERSITY OF MALAYA
KUALA LUMPUR**

2012

**IMPROVEMENT OF THE PROCESSING OF INITIAL CONDITIONS OF
PARTICLES UNDERGOING DEP EFFECTS IN HOMOGENOUS
SUSPENSION USING MATLAB**

NOOR HIDAYAH BT. AMIR HASSAN

RESEARCH REPORT SUBMITTED

**IN PARTIAL FULFILMENT OF THE REQUIREMENT FOR THE DEGREE
OF MASTER OF ENGINEERING (BIOMEDICAL)**

2012

ABSTRACT

Cell separation and manipulation are currently becoming highly purposeful due to its function variation and becoming possible due to the availability of dielectrophoresis (DEP) method. Commonly used in cancer cell detection and drug screening assessment, DEP are able to manipulate polarisable particles with the application of non-uniform electric considering the fact that movement will be induced onto the polarisable particles when placed in the electric fields. The application of DEP are used to be restricted in research for academic prospects only, rather than in manufacturing applications due to the laborious and time-consuming processes involved, but recently with the existence of multi-channels microelectrode array, real-time assessment of cell populations are accredited since each electrodes were being energized individually with desired voltage, frequency and phase. The physiological characteristics of cell populations are being extracted from DEP spectrum which was obtained from image processing technique which previously involves histogram-based algorithm and CMIS method. The current research attempts to introduce new method of determining the distribution of cells to be even or not. This is crucial in multiple dot system but not so much important for single dot system. This is because the algorithm developed based on CMIS and histogram plots are already proven to be effective. The proposed method named average counts attempt to manipulate the average grey level values of each pixels and standard deviation plot obtained is used to draw the conclusions from the findings.

ABSTRAK

Pemisahan serta manipulasi sel semakin berguna di masa kini disebabkan oleh fungsinya yang berkepelbagaian dan semakin mudah dilakukan sejak meluasnya aplikasi teknik Dielektroforesis (DEP). Sejak belakangan ini, DEP semakin banyak digunakan di dalam proses mengesan sel-sel kanser and ujian pengesanan ubat-ubatan serta dadah. Ini adalah kerana kebolehan DEP memanipulasikan zarah-zarah bersifat cas dengan mengenakan arus elektrik yang tidak sekata akan menghasilkan pergerakan zarah-zarah tersebut. Kegunaan DEP dahulunya terhad hanya kepada kajian dalam bidang akademik sahaja disebabkan oleh masa yang diambil untuk menyelesaikan satu eksperimen adalah sangat panjang dan memerlukan kerja-kerja makmal yang banyak. Tetapi sekarang, ianya bertambah mudah dengan kehadiran elektrod beberapa-salur. Elektrod beberapa-salur ini digunakan untuk menganalisa populasi sel secara terus disebabkan oleh setiap salur itu dibekalkan dengan arus elektrik secara berasingan dengan nilai arus, voltan, fasa dan frekuensi yang berbeza-beza. Sifat-sifat elektrofisiologi untuk sesuatu populasi sel boleh didapati daripada DEP spectrum yang dikeluarkan daripada analisa gambar. Teknik yang sudah lama digunakan ialah teknik CMIS dan graf histogram. Buat masa sekarang, teknik terbaru telah diperkenalkan untuk menentukan samaada suatu gambar itu mempunyai taburan sel dengan sekata atau pun tidak. Ini penting untuk elektrod beberapa-salur tetapi tidak begitu penting untuk elektrod satu-salur kerana untuk satu-salur, CMIS dan graf histogram telah membuktikan kebolehan untuk mentafsirnya dengan begitu baik skali. Teknik terbaru ini bernama kiraan purata yang menggunakan nilai hitam putih yang ada dalam piksel dan sisihan piawai digunakan untuk menghasilkan kesimpulan yang munasabah daripada keputusan yang dijumpai.

UNIVERSITI MALAYA

ORIGINAL LITERARY WORK DECLARATION

Name of Candidate: **NOOR HIDAYAH BT. AMIR HASSAN**

(I.C/Passport No: **880111-07-5020**)

Registration/Matric No: **KGL 100006**

Name of Degree: **Master of Engineering (Biomedical)**

Title of Project Paper/Research Report/Dissertation/Thesis ("this Work"):

IMPROVEMENT OF THE PROCESSING OF INITIAL CONDITIONS OF PARTICLES UNDERGOING DEP EFFECTS IN HOMOGENOUS SUSPENSION USING MATLAB

Field of Study: **DIELECTROPHORESIS**

I do solemnly and sincerely declare that:

- (1) I am the sole author/writer of this Work;
- (2) This Work is original;
- (3) Any use of any work in which copyright exists was done by way of fair dealing and for permitted purposes and any excerpt or extract from, or reference to or reproduction of any copyright work has been disclosed expressly and sufficiently and the title of the Work and its authorship have been acknowledged in this Work;
- (4) I do not have any actual knowledge nor do I ought reasonably to know that the making of this work constitutes an infringement of any copyright work;
- (5) I hereby assign all and every rights in the copyright to this Work to the University of Malaya ("UM"), who henceforth shall be owner of the copyright in this Work and that any reproduction or use in any form or by any means whatsoever is prohibited without the written consent of UM having been first had and obtained;
- (6) I am fully aware that if in the course of making this Work I have infringed any copyright whether intentionally or otherwise, I may be subject to legal action or any other action as may be determined by UM.

Candidate's Signature

Date

Subscribed and solemnly declared before,

Witness's Signature

Date

Name:

Designation:

ACKNOWLEDGEMENT

Bismillahirrahmaanirrahim. Lots of syukur and praises to Allah the Almighty, whom without Him, none of this would have been made possible. Throughout the preparation of this dissertation, I would like to express my full gratitude to my dearest parents, Amir Hassan b. Abdul Wahid and Rahimah bt. Packer Mohamed, for their undying support and sacrifices from the beginning of my study until the end. I could never have done it without them by my side. To my beloved husband Mohd. Hafiz b. Zakaria, thank you for being highly understanding for my long-term absence during times you needed me. I am deeply indebted to my highly supportive supervisor, Dr. Nahrizul Adib b. Kadri for all the help, stimulating suggestions and encouragement that have guided me all the time through the research. I would like to express my gratitude to all my study group members, whom have always been so supportive and willing to assist at any time in need. Also to Faiz Saaid, who have been most generous with the knowledge of programming and was not a littlest bit stingy about sharing it. All the welcoming gestures, smiling faces, and friendly treatment greeted me each time I went to the lab. None of it will ever be forgotten. To all my classmates, the students of Biomedical Engineering master students, I will always remember all the warm support and motivation offered at all times.

My sincerest appreciation also extends to all who have provided assistance at various occasions. This piece of gratitude also extends to all my family members who have been very supportive to me. Thank you all.

TABLE OF CONTENTS

| CHAPTER | TITLE | PAGE |
|----------|--|------|
| | TITLE PAGE | i |
| | ABSTRACT | ii |
| | ABSTRAK | iii |
| | DECLARATION | iv |
| | ACKNOWLEDGEMENTS | v |
| | TABLE OF CONTENTS | vi |
| | LIST OF TABLES | vii |
| | LIST OF APPENDICES | vii |
| | LIST OF ABBREVIATIONS | vii |
| | LIST OF FIGURES | viii |
| 1 | INTRODUCTION | |
| | 1.1 Overview | 1 |
| | 1.2 Research Objectives | 4 |
| | 1.3 Organization of Thesis | 5 |
| 2 | LITERATURE REVIEW | |
| | 2.1 Background of Study | 6 |
| | 2.2 Theory | 7 |
| | 2.3 Development of Algorithm | 11 |
| | 2.4 Analysis of DEP images | 14 |
| 3 | METHODOLOGY | |
| | 3.1 Experimental Setup | 19 |
| | 3.2 Improvement on Image Analysis | 21 |
| 4 | RESULTS AND DISCUSSION | |
| | 4.1 Results and Discussion | 26 |
| 5 | CONCLUSIONS AND RECOMMENDATIONS | |
| | 5.1 Summary | 33 |
| | 5.2 Limitation | 34 |
| | 5.3 Future Recommendations | 34 |
| | REFERENCES | 35 |
| | APPENDIX A | 37 |

LIST OF TABLES

| TABLE NO. | TITLE | PAGE |
|------------------|--|-------------|
| 2.1 | Results of an example of the proposed analysis of the initial captured image | 21 |
| 3.1 | Segmented dots from the original image | 28 |
| 4.1 | Pixel segment vs. standard deviation plot for images with even distribution of cells | 34 |
| 4.2 | Pixel segment vs. standard deviation plot for images with uneven distribution of cells | 36 |

LIST OF APPENDICES

| APPENDIX NO. | TITLE | PAGE |
|---------------------|--------------------------------|-------------|
| A | MATLAB code for average counts | 42 |

LIST OF ABBREVIATIONS

| | |
|------|------------------------------------|
| DEP | - Dielectrophoresis |
| CMIS | - Cumulative Modal Intensity Shift |
| LOC | - Lab-on-chip |
| AC | - Alternating current |
| ROT | - electrorotation |
| ROI | - Region of interest |

LIST OF FIGURES

| FIGURE NO. | TITLE | PAGE |
|------------|--|------|
| 2.1 | A schematic diagram of a positive DEP effect (particle is more polarisable than the surrounding medium). | 10 |
| 2.2 | A typical shape of a DEP spectrum | 12 |
| 2.3 | Flowchart of the algorithm for detecting the initial intensity level of the captured images | 16 |
| 3.1 | Pre-analysis showing (a) before and (b) after elimination of electrodes | 25 |
| 3.2 | Flowchart of the whole process | 26 |
| 3.3 | The process of elimination of non-profitable areas | 27 |
| 3.4 | Development of horizontal and vertical strips | 29 |
| 3.5 | Magnified image of the process of dot extraction from an initial image | 30 |
| 4.1 | Classifying pixels into pixel segments | 33 |
| 4.2 | Standard deviation plots o the first group of images with evenly distributed cells | 39 |
| 4.3 | Standard deviation plots o the first group of images with evenly distributed cells | 39 |

CHAPTER 1

INTRODUCTION

1.1 Overview

Integration of numerous lab functions into a single-chip component with miniaturized size is crucial in conducting experiments which deals with micro-to-nano-sized particles such as cancer cells, bacteria or viruses. The existence of these devices enables laboratory-on-a-chip came into life and assists the examination process of miniature-sized cells. The conventional technology behind lab-on-a-chip (LOC) was implemented into the functional microelectrodes which were adopted from photolithographic techniques that were developed by the semiconductor industries (Hughes, 2002; Crane, 1968).

Dielectrophoresis is the phenomena where interactions between polarized particles with non-uniform electric fields exert motion onto the particles. It can be used and adopted to manipulate, separate, and analyze the cellular and viral particles responses (Hubner *et al.*, 2007; Hoettges *et al.*, 2008; Pethig, 2010). The induced motion and the manipulation of particles which have been polarized after being suspended in a non-uniform alternating electric field can cause repulsion or attraction of cells with regards to the electrodes.

DEP has become recognizable since its introduction which defines DEP as “the motion of suspensoid particles relative to that of the solvent resulting from polarization

forces produced by an inhomogeneous electric field” (Pohl, 1951). One of the advantages of DEP is that it does not need chemical markers, biochemical labels or bioengineered tags and at the same time does not exert any contact to any surfaces of cells making this technique preferable compared to chemical method such as fluorescent labels which are highly invasive and cell destructive (Hoettges *et al.*, 2008; Pethig, 2010).

There are a few major contributions of DEP-based technique especially in distinguishing dead and viable cells by separating and sorting them according to its conductivity of the cytoplasm, surface charge and the capacitance of the membrane. This is proven by a study done by Gascoyne *et al.* (1992) which demonstrate the separation of cancer cells on an electrode array due to the differences in terms of frequency shown between normal, leukemic and differentiation-induced leukemic mouse erythrocytes (Gascoyne *et al.*, 1992). This is further being supported by Becker *et al.* (1994 & 1995) who found and exploited the differences in the dielectric properties of metastatic human breast cancer cell from those of erythrocytes and T-lymphocytes resulting in the separation of breast cancer cells from the normal blood cells (Becker *et al.*, 1995; Becker *et al.*, 1994).

In another study by Wang *et al.* (2002) authenticated that the membrane dielectric properties changes of HL-60 (cultured human promyelocytic leukemic cells) been detected by using DEP in the early stage of apoptosis after treatment with genistein compound (Wang *et al.*, 2002; Labeed *et al.*, 2006). All these achievements came down to the analysis and correlation between dielectrophoretic force (F_{DEP}) with the physical phenomena which can be observed by the aid of video cameras or fluorescent chemical markers. With the application of non-uniform alternating current (AC) electric fields, polarisable particles such as cells will become polarized when being suspended in the said electric fields.

Suspension of dielectric particles, particularly cells in an electric field will result in polarization of particles and the direction of the induced dipole is dependent of frequency and magnitude of the said electric field. Microelectrodes, where the electric field is originated will generate a gradient of fields which determines the classification of the DEP, positive or negative, based on the direction of movement of cells with respect to the electric field gradient and the induced dipole. These series of events was captured and recorded using video cameras and the image was analyzed using image processing technique in order to extract useful DEP information particularly electrophysiological properties of cells by interpreting the frequency-dependent movement of cells, which also known as DEP spectrum (Fatoyinbo *et al.*, 2008; Lee *et al.*, 2004; Labeed *et al.*, 2003).

Before the captured images can be analysed and the corresponding DEP spectrum be plotted, segmentation of the actual dots within the image must be completed. The segmentation algorithm will generally conduct two main processes, namely the production of a layer mask to distinguish between the electrodes and the dots based on a chosen intensity threshold value, and the detection of bona fide dots based on the similarities of the area sizes. The measured values of the extent of the cellular movement under the DEP influence will then be normalised and employed in the construction of the corresponding DEP spectrum.

The algorithm for the relative polarisability measurement was based on the Cumulative Modal Intensity Shift (CMIS) image analysis technique that was developed for use with single dot planar microelectrode system with 4-by-4 dot array design while not allowing each dot to be energized separately (Fatoyinbo *et al.*, 2008). As the name CMIS suggests, this method relied on the modal value of the histogram of the captured images. Generally, the algorithm will first detect the modal value by finding the peak of the histogram, and subsequently will sum the total number of pixels starting from this

point onwards to the maximum light intensity value of the histogram. The parallel system has been developed by Fatoyinbo *et al.* (2011) which allow each dot in the electrode array to be energized individually and simultaneously with various frequencies (Fatoyinbo *et al.*, 2011).

1.2 Research Objective

There are a few main concerns that this research is thoroughly focused on. As a sequel of previous research done by Kadri (2010), this sort project provides an optimization in the technique used to analyze the initial image prior conducting an experiment. This is previously done manually by being fully dependent on user expertise with no automated system to verify the eligibility of a certain image to proceed through to experimental level, thus affecting the results produced by the experiment and making the results questionable. The process of introducing an automated system for this matter is still new in the academic arena and is only crucial for multiple dots system. This is because, for single dot system, the algorithm developed by Fatoyinbo *et.al* (2008) has been established and have proven to be working just fine. We make it our aim to pioneer the development of an automated system that can achieve this objective. Other than that, with the application of the new system, statistical analysis is also made as a main objective to verify the level of effectiveness of this method. Thus, the real objective of this project is to propose a new automated system, which is the average count method, as a method of verifying the eligibility of a particular cell distribution to proceed to the experimental level.

1.3 Organization of Thesis

This thesis consists of five chapters. These chapters discuss about the introduction, literature review of study, methodology, discussions of results and conclusions with recommendations for future study. Chapter 1 discusses briefly about the DEP experiments and its procedures as a whole. The objectives of the research are also being explained in this chapter. In the next chapter which is Chapter 2, it shows the literature review which consist of the background of study, the theory of DEP phenomenon, the development of algorithm and the analysis process which have been previously adopted for image analysis. Chapter 3 describes the procedure of the analysis and its experimental setup. In addition to that, the improvement of image analysis technique was also introduced in this chapter. Chapter 4 discusses the results obtained from the analysis and last but not least the conclusions along with the limitations of the research and some recommendations were discussed in Chapter 5.

CHAPTER 2

LITERATURE REVIEW

2.1 Background of Study

Dielectrophoresis (DEP), along with electrorotation (ROT) (Hughes, 2002; Lee *et al.*, 2004; Gascoyne *et al.*, 20) is frequently grouped as a member of AC-electrokinetic technique which manipulates the mobility of cells in an electric field with non-uniformity and time-dependent properties in order to explore the electrophysiological properties of cells (Hughes, 2002; Jones *et al.*, 2003; Jones, 2003; Jones, 1995; Pethig *et al.*, 1997; Pohl *et al.*, 1981). Important information can be extracted from the electrophysiological properties especially at the cellular level. DEP method is known to be inevitably nondestructive and noninvasive, while being a label-free cell characterization technique when compared to the chemical methods which results in invasion of cellular trafficking or compared to electrical measurement method as such patch clamp which is highly destructive to cells (Labeed *et al.*, 2003).

Since its discovery by Herbert Pohl in 1951, DEP has been adopted in experiments for separating nonviable and viable yeast cells (Crane, 1968; Pohl, 1966). Thereafter, many more studies have emanated with mostly exploiting towards different fields such as the characterization and diagnostic techniques for cancer cells (Broche *et al.*, 2007), the earlier detection of changes in dielectric properties on cell membrane

(Wang *et al.*, 1994), the resistance factor of chemotherapy by cancer cells lines (Labeed *et al.*, 2003), detection of oral cancer and malfunction (Broche *et al.*, 2007) and the biophysical changes in apoptosis-induced leukemic cells (Chin *et al.*, 2006). Other than that, there are also studies done to separate bone marrow from blood (Yang *et al.*, 1999). Although numerous studies have proven the viability of the technique, DEP has yet to be accepted worldwide, especially commercial-wise due to the time consuming and laborious procedures.

2.2 Theory

The phenomenon of dielectrophoresis (DEP) refers to the translational movement of particles due to the interactions between an induced dipole and a non-uniform alternating electric field. Depending on the overall alignment of the induced dipole moments, the particles will either move towards or away from the area with the highest electrical gradient (Hughes, 2002; Jones, 1985). The dipole alignment is determined by the relative polarisability of the compared to the surrounding medium. The direction of the overall force however, does not depend on actual direction of the electric field.

There are two types of DEP namely positive and negative. The phenomena of positive DEP occur when the particle is more polarisable than the surrounding medium which will then causing induction of dipole moment on its surface. Due to the high electrical gradient towards the negative end, the particle will then experience a net force towards it as expressed in Figure 2.1. While for negative DEP, the effective motion of particle is totally dependent on the polarisability of the particle and its medium, rather than the gradient of electric field. This is because during negative DEP, the surrounding

medium happens to be more polarisable than the particle, and thus repelling the particle towards the positive end of the gradient.

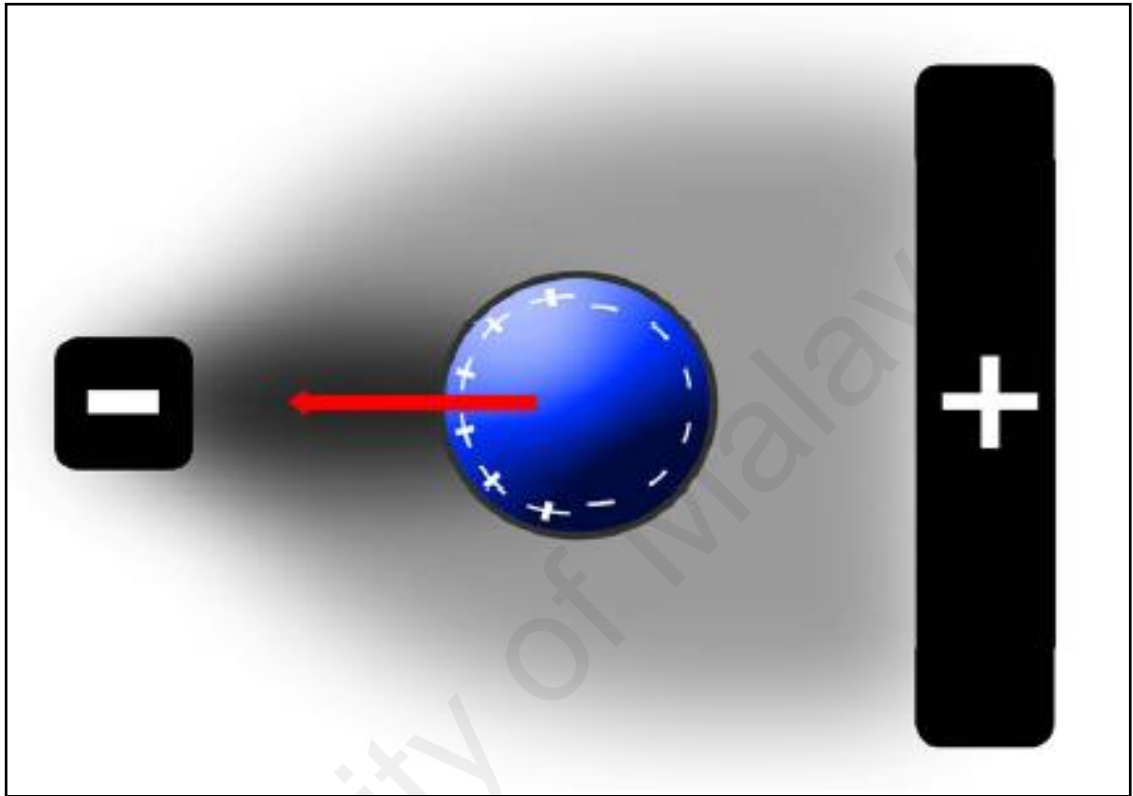


Figure 2.1 : A schematic diagram of a positive DEP effect (particle is more polarisable than the surrounding medium). Red arrow indicates the net motion of the particle.

By taking the assumption of a cell or particle being the shape of a sphere, the DEP force can be deduce as

$$F_{DEP} = 2\pi r^3 \epsilon_m \text{Re}[K(\omega)] \nabla E^2 \quad \text{Eq. 1}$$

where r is the radius of cell, ϵ_m is the permittivity of medium in the surrounding area, $K(\omega)$ is the complex Clausius-Mossotti factor, ∇ is the gradient operator, E is the strength or amplitude of the electric field in RMS value.

$$K(\omega) = \frac{\epsilon_p^* - \epsilon_m^*}{\epsilon_p^* - 2\epsilon_m^*} \quad \text{Eq. 2}$$

$K(\omega)$ is the Clausius-Mossotti factor which have a huge influence on the overall effective polarisability of particles. In the above equation, ε_p^* and ε_m^* are the complex permittivities of cell and medium, respectively.

In addition to that,

$$\varepsilon^* = \varepsilon - \frac{j\sigma}{\omega} \quad \text{Eq. 3}$$

where σ refers to the conductivity of the medium, ε refers to the permittivity and ω is the angular frequency of the of the applied AC electric field.

In the F_{DEP} equation from (Eq. 1), the existence of Clausius-Mossotti factor, which is a frequency-dependent element, ensures that the F_{DEP} also varies with the frequency of the applied electric field. The factor relies upon the strength of the relative polarisability between the particle and the surrounding medium. If the factor is positive, it reflects that the particle is more polarized than the medium, thus effective motion will results in moving towards the area with the highest gradient of electric field. Opposing to this, when a negative DEP befall and the medium is more polarisable than the particle, the effective motion will result in repelling of particle towards the lower gradient of electric field. This will happen when the Clausius-Mossotti factor brings out a negative value.

In order to enable the dielectric properties to be directly calculated and correlated in a useful manner, the above analytical expressions are needed to be expanded. There are complexities faced while trying to do so even though the analytical expressions may have explained thoroughly the DEP behaviour of spheres in a medium. By performing the best-fit numerical analysis, an estimation of electrophysiological properties can be made to correlate the relevant cellular electrical parameters with DEP behaviour.

The estimation method has also shown to be very useful in characterizing multiple cell populations within a heterogeneous cell sample (Chin *et al.*, 2006; Huang *et al.*, 1996; Broche *et al.*, 2005). A DEP spectrum has proven to be very beneficial in the extraction of electrophysiological properties because it also provides the estimation of the state and environment surrounding the cells.

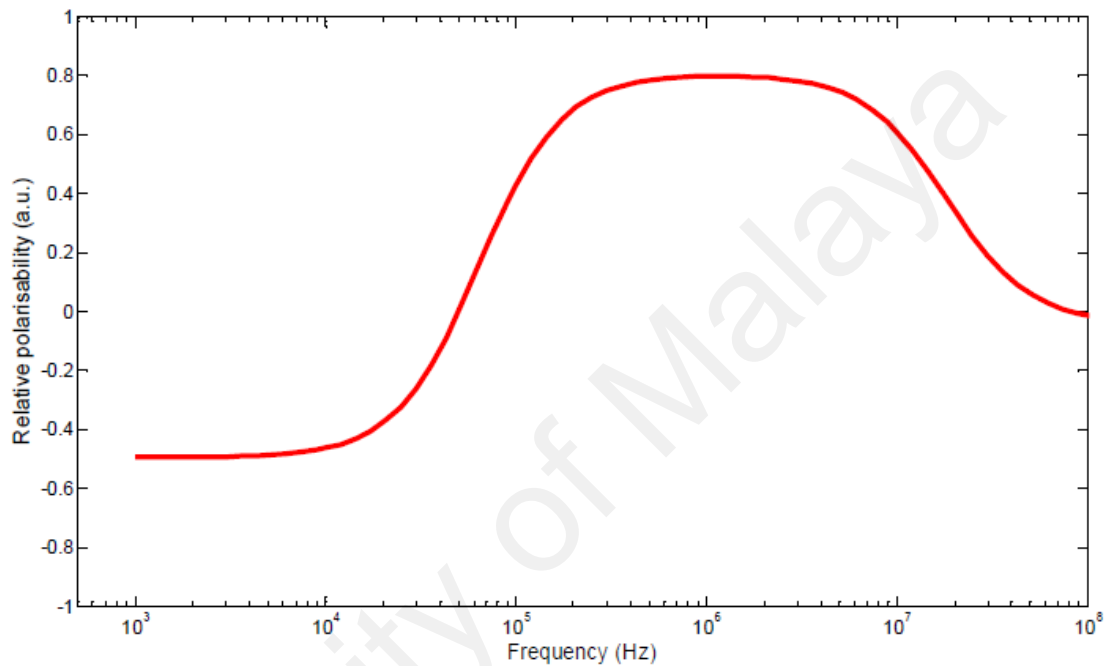


Figure 2.2: A typical shape of a DEP spectrum

Figure above shows the typical shape of the DEP spectrum while it can be shifted both ways, either to the right or to the left, depending on a particular influence that an external reagent has on the Clausius-Mossotti factor. This is due to the changes in components of Eq. 2 which consist of conductivity, permittivity, and angular frequency. A close example of this effect would be when an ionophore molecules were attached to the cellular membrane, higher level of ions were allowed to pass through the membrane which ultimately disturb the conductivity thus disturbed the ionic distribution. This will in turn disturb the Clausius-Mossotti factor value and result in a frequency shift of the DEP spectra.

2.3 Development of algorithm

The algorithm adopted for this experiment originated from the basic dielectrophoretic force (F_{DEP}) in Eq. 1 as mentioned in previous section, which represents the displacement of particles under the influence of non-uniform AC current electric fields.

$$F_{DEP} = 2\pi r^3 \epsilon_m \text{Re}[K(\omega)] \nabla E^2 \quad \text{Eq. 1}$$

where ϵ_0 is the permittivity of the free space, ϵ_m is the permittivity of the suspending medium, r is the radius, E is the electric field and $\text{Re}[K(\omega)]$ is the real part of the Clausius-Mossotti factor, which is a frequency-dependent value, exhibited by Eq. 2 below, where ω is the angular frequency, and ϵ_p^* and ϵ_m^* are the complex permittivity of the particle and suspending medium respectively.

$$\text{Re}[K(\omega)] = (\epsilon_p^* - \epsilon_m^*) / (\epsilon_p^* + 2\epsilon_m^*) \quad \text{Eq. 2}$$

Being a frequency-dependent value, the real part of the Clausius-Mossotti factor plays a major role in determining the direction of the particle movement other than the polarisability of particles and suspending medium. Attraction and repulsion of particles with respect to the electric field generated by the electrode will determine the type of DEP the particles are experiencing. Attraction to the electrode is called positive DEP and repulsion from the electrode is called the negative DEP. From the experiment, images captured were analysed and it is found that the image processing technique, which is the histogram-based analysis, gives a much better option than the manual mathematical approach by using numerical method.

Since the algorithm in the current analysis relies upon the histogram of light intensity in the captured images, it is of utmost importance therefore that the quality of the images is at the required optimal level. The contrast and brightness of the image,

prior to conducting the experiment, must be set accordingly for the subsequent analysis to be completed. The analysis particularly requires that the image must not be too dark or too bright, in order for it to correctly detect the dots and later to complete the analysis of the histogram within each of the dots.

In the current program however, there is not a facility to quantify the level of contrast and/or brightness of the captured image, thus leaving it entirely to the judgement of the user to decide if the light intensity and the focusing of the microscope lenses were optimum. An ideal additional feature to the program would be a facility to automatically capture the contrast and brightness levels of the captured image, and use those values to automatically adjust the camera settings that allow it to capture the best images for the purpose of analysis. This approach however, requires additional programming that must interface with the digital camera, which is both time-consuming and demands high computing resources. In addition, any adjustment on the camera settings relies on the light intensity level coming from the microscope anyway, thus still requiring the subjective input of the user to a certain extent. An additional difficulty is in determining the uniformity of cell distribution over the dots, since the analysis algorithm relies on the light intensity coming through each of the individual dots.

A simpler approach is therefore proposed to address both of the said problems in the current program, whereby it allows a user to quickly determine if the captured images are within the optimal range of contrast and brightness, and if the cells are distributed uniformly over each of the dots, prior to starting an experiment. If the captured images were not at its optimal starting conditions, the user simply have to adjust the light intensity of the microscope and/or re-suspend the cells within the chamber, and restart this additional feature of the program. Figure 2.3 below shows the flowchart of the algorithm for this feature.

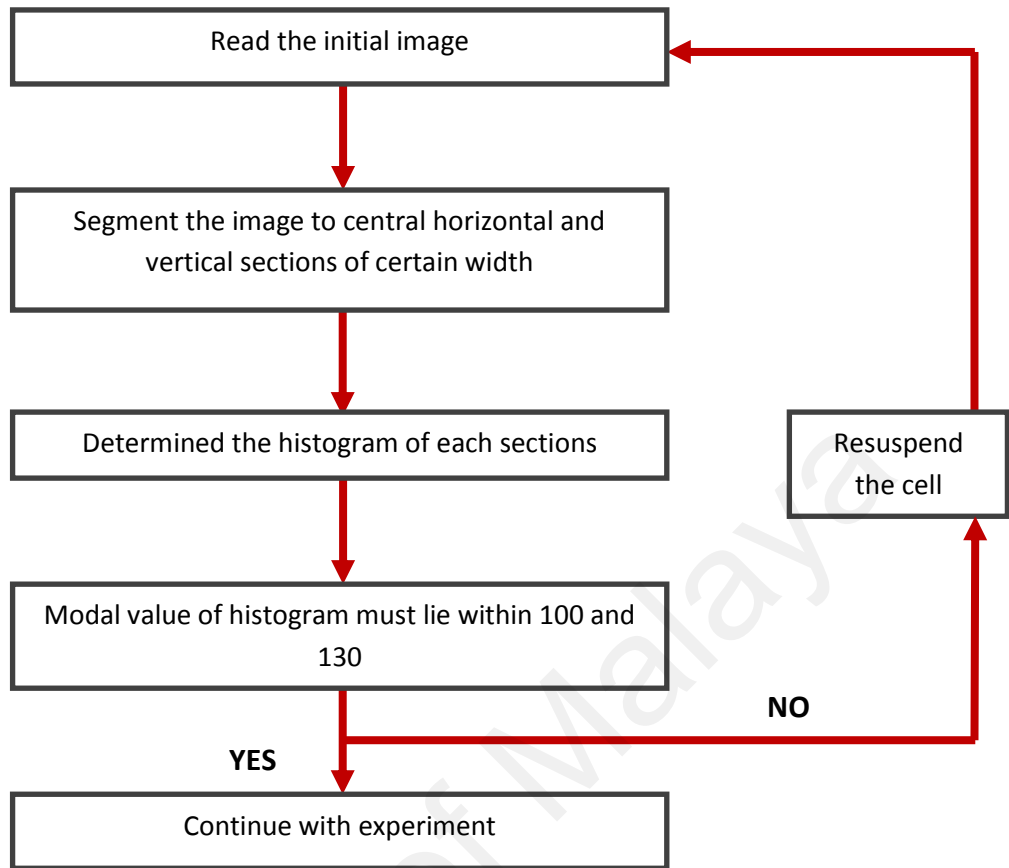


Figure 2.3: Flowchart of the algorithm for detecting the initial intensity level of the captured images

As shown in the flowchart, the chosen indicator for the additional feature is the modal value of the histogram of each dot. This is primarily due to the finding that the majority of dots that provide satisfactory cell distribution and subsequently good DEP spectra have its modal histogram value within the same region of intensity. Following an examination of 112 dots that fulfils the said criteria, it was found that the modal intensity level is $127.76 (\pm 15.45)$.

Therefore, it is proposed that the rounded intensity values of between 100 and 130 be used as an indicator to determine that the captured images have the optimal contrast and brightness required for the subsequent analysis. It was also found that a uniformly distributed cells within a given dot gave similar histogram plots, particularly values for maximum and minimum intensity levels, and the height (corresponding to total number of pixels at a particular intensity level) of the plot.

2.4 Analysis of Dielectrophoresis (DEP) Images

The basic theory behind cumulative modal intensity shift (CMIS) method is to manipulate the possible relationship established between the Clausius-Mossotti factor and the cellular concentration shift for a population under the observation of a microscope, by adopting the Beer-Lambert's law of light absorption. In the adaptation of CMIS method, a Beer-Lambert region must be defined beforehand. If the region is defined to be at the center of the dot, this will narrow down the region of evaluation of light intensity.

From the chosen Beer-Lambert's region, attraction and repulsion of cells from the dot perimeter, where the source of electric field came from, will cause changes in light intensity coming through the defined region. For example, negative DEP, which results from the repulsion of cells from the area with high DEP force, will generate an accumulation of cells at the center of the dot. This will in turn limit the light intensity coming through that particular region.

On the contrary, the positive DEP which results in the attraction of cells towards the dot perimeter where the highest DEP force is exerted will allow greater amount of light to be transmitted through that particular region. Quantification of the Clausius-

Mossotti factor is made by comparing the changes in the light intensity values between the captured images at a certain time frame with the reference image at the initial stage of the experiment.

In previous study (Fatoyinbo *et al.*, 2008), the dot system was used to quantify the DEP force which in turns will determine the polarisability of the cells of interest. The relationship between the shifts in particle concentration with time can be established by applying the Beer-Lambert's law of light intensity, thus, the Clausius-Mossotti factor. Assuming that initially, the dispersion of cells is uniform and the initial light intensity to be I_0 , the final state of light intensity (I) will be proportional to the concentration shifts of cells or particles in response to the applied DEP force. Intensity, I , tend to revolve depending on the cells accumulation as such in the middle due to repulsion of cells from the dot perimeter (negative DEP) which will decrease the light intensity and vice versa. This event can be expressed by Eq. 4:

$$I = I_0 e^{-A\Delta z C} \quad \text{Eq. 4}$$

where C is the concentration of cells, A is the area, and Δz is the total path length of light. It is shown in a study done by Fatoyinbo *et al.* (2008) that the concentration difference over a specific volume is proportional to the average particle velocity, which in turn is proportional to the dielectrophoretic force and the Clausius-Mossotti factor as expressed in Eq. 5:

$$\frac{d(\ln(I/I_0))}{dt} \propto |\bar{F}_{DEP}| \propto \text{Re}[K(\omega)] \quad \text{Eq. 5}$$

where $\text{Re}[K(\omega)]$ is the real part of Clausius-Mossotti factor, \bar{F}_{DEP} is the DEP force. In order to calculate the CMIS, two types of region of interest (ROI), namely center and outer region was introduced and identified in the dot aperture to be a third of the distance along the radius from the dot center. Cumulative pixels intensity values of the

initial and after image were compared to each other. Since the images were digitized pixel by pixel and quantized using an 8-bit unsigned greyscale spectrum, the intensity value (P) was defined to be between 0 and 255 ($0 \leq P \leq 255$) which represents black and white respectively. With the values clearly defined, needless to say that during negative DEP, the cumulative pixel intensity value at the center region of the after image (I_{after}) will decrease if compared to the initial image intensity (I_{initial}) due to the collection of cells that are centered in the middle of the dot, therefore limiting light to pass through. Opposing from negative DEP, positive DEP will produce higher image intensity in the after image (I_{after}) compared to the initial image (I_{initial}).

Generally, a histogram computes the distribution of intensities in a greyscale image which can further be used in image enhancement operation. It will count and sort all pixels with common intensity values. It is obvious that the histogram plot is relevant to the post-study of a DEP experiment due to the fact that when the cells are experiencing negative DEP, the histogram plot shows huge proportion of low pixel values (darker pixels) while huge proportion of high pixel values (brighter) was produced when the cells are in positive DEP experience. The cumulative values of pixels when counted from the modal values, which is the histogram peak, upwards towards the spectral maximum would shift to negative and positive values for negative and positive DEP respectively when compared and normalized against the values of an initial image.

The findings from previous study by Kadri (2010) were discussed briefly. Extraction of useful DEP information from the captured image starts with measuring the extent of cellular movement under the DEP influence in order to quantify the relative polarisability of the cell populations in use. These measured values will be normalized and employed in the construction of the corresponding DEP spectrum. The algorithm for the relative polarisability measurement was based on the Cumulative Modal

Intensity Shift (CMIS) image analysis technique that was developed for use with single dot planar microelectrode system (Fatoyinbo *et al.*, 2008). As the name suggests, this method relied on the modal value of the histogram of the captured images. Generally, the algorithm will first detect the modal value by finding the peak of the histogram, and subsequently will sum the total number of pixels starting from this point onwards to the maximum light intensity value of the histogram.

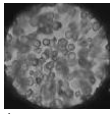
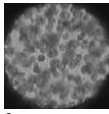
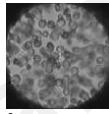
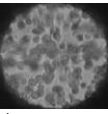
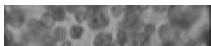
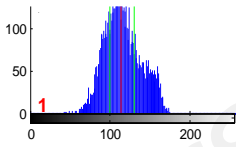
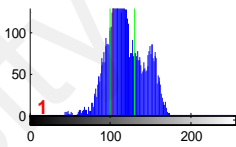
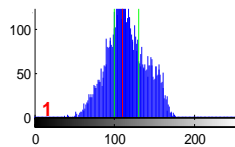
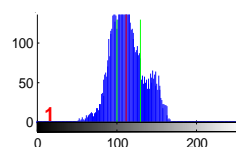
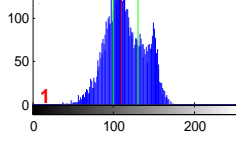
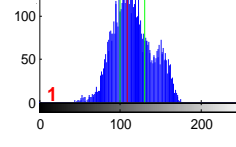
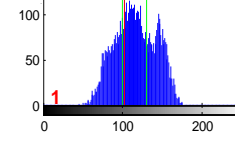
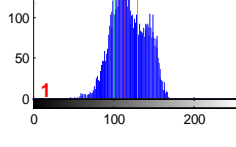
| | Image 1 | Image 2 | Image 3 | Image 4 |
|-------------------------------------|---|---|---|---|
| Full view of image |  |  |  |  |
| Horizontal strips |  |  |  |  |
| Histogram plot of horizontal strips |  |  |  |  |
| Verticle strips |  |  |  |  |
| Histogram plot of verticle strips |  |  |  |  |

Table 2.1: Results of an example of the proposed analysis of the initial captured image

Since the images was captured using an 8-bit greyscale spectrum, therefore will have values ranging from 0 (black) to 255 (white). The histogram of the captured images will count and sort all pixels with common intensity values. Table 2.1 above display the results shown in terms of histogram plots of the four different images taken during the experiment in order to obtain the DEP spectra of biological cells. The first row shows the full view of the dot image while row 2 and 4 shows the segmented central horizontal and central vertical strips from the original image respectively. From these strips, each of the histogram plots was generated by the additional module that analyses the captured initial image of the four-dot system. It is noted that each of these dots have scored a '1' for both horizontal and vertical central strips which implies that the distribution of cells within each dots were uniform and the modal value of the histogram level (red line) lies within the proposed optimum boundary levels (green lines). As mentioned in the flow chart in Figure 2.3, it is predetermined that the maximum and minimum modal values of the histogram were to be between 100 and 130 and as proven by the analysis, the results of each histogram modal values does fulfil the said boundaries. This further implies that the image has optimum contrast and brightness for it to be efficiently analyzed.

CHAPTER 3

METHODOLOGY

3.1 Experiment Setup

From previous research experiments done by Kadri (2010), images of cells in electrodes prior starting an experiment are collected and provided for this research. Previously in the experiment, video cameras were placed above the electrodes containing the cells in order to record the progress of cells throughout the experiment. With the help of the video camera, images were taken at the frequency of 10 pictures per second.

The pictures were then analyzed at the initial stage of the experiment, which is at $t=0$. This is crucial in determining the suitability of a specific cell population distribution to proceed to the experimental level. Previously done by Kadri (2010), the initial image was analyzed by applying histogram plots for each dot image. Prior to this, the dots were segmented out from the whole image in order to enable analysis on each dot can be done. The process generally involves differentiating between the electrodes and the dots, thus improving the viability of the results instead of taking the whole picture. The process is briefly described in the figure. Through this process, the electrodes were eliminated from the whole picture due to the fact that it is of no purpose for the analysis. This is the pre-step of the analysis which will have to be done first prior starting and analysis of the image.

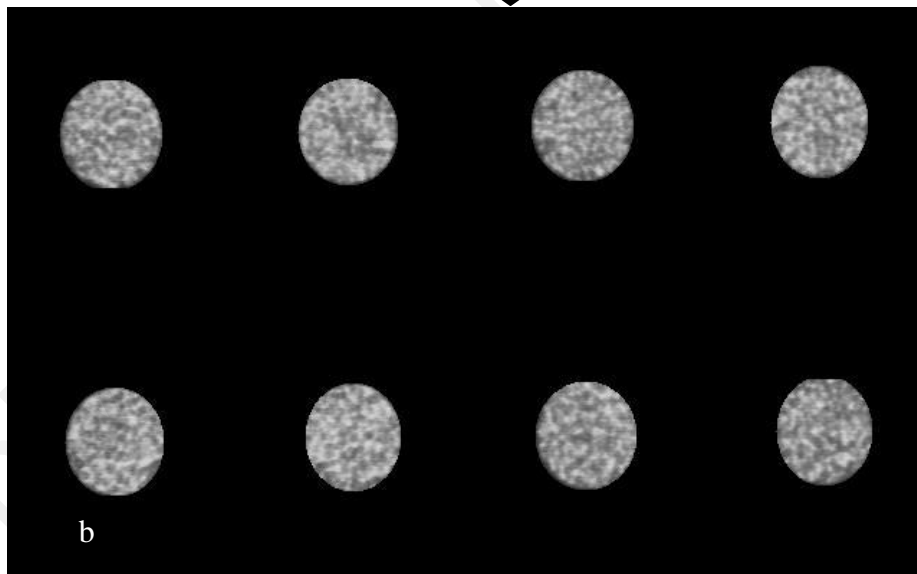
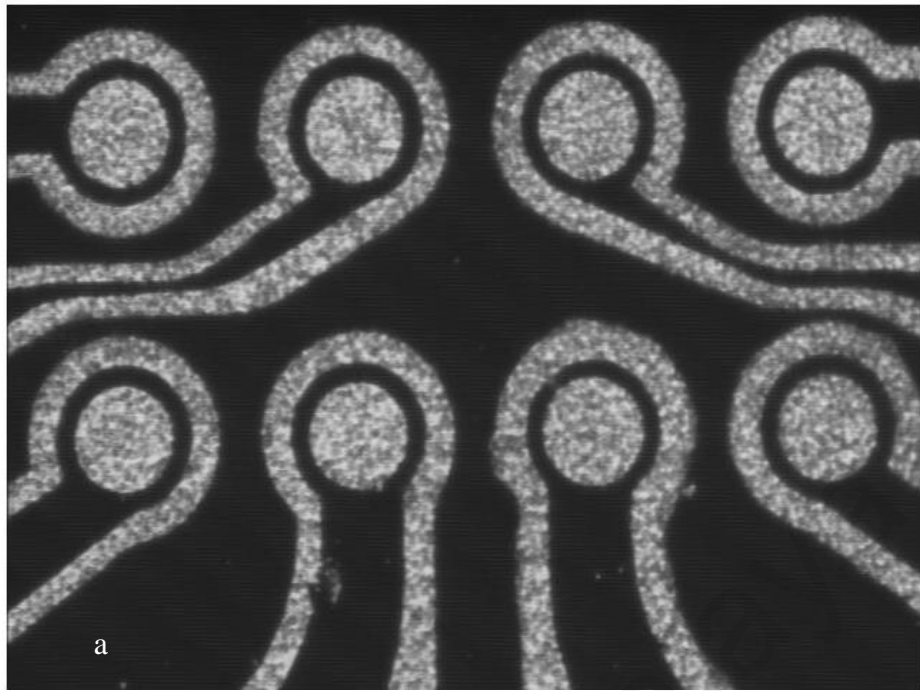


Figure 3.1: Pre-analysis showing (a) before and (b) after elimination of electrodes

3.2 Improvement on Image Analysis by using Average counts method

The main objective of this research is to optimize the way of analyzing initial images prior starting an experiment. In the support of histogram plots technique and CMIS technique mentioned in Chapter 2, average counts of grey levels is proposed to have a beneficial effects. This is analysis is made possible with the help of MATLAB program where the coding n programming were done. The steps involved for this improvement technique is summarized in below.

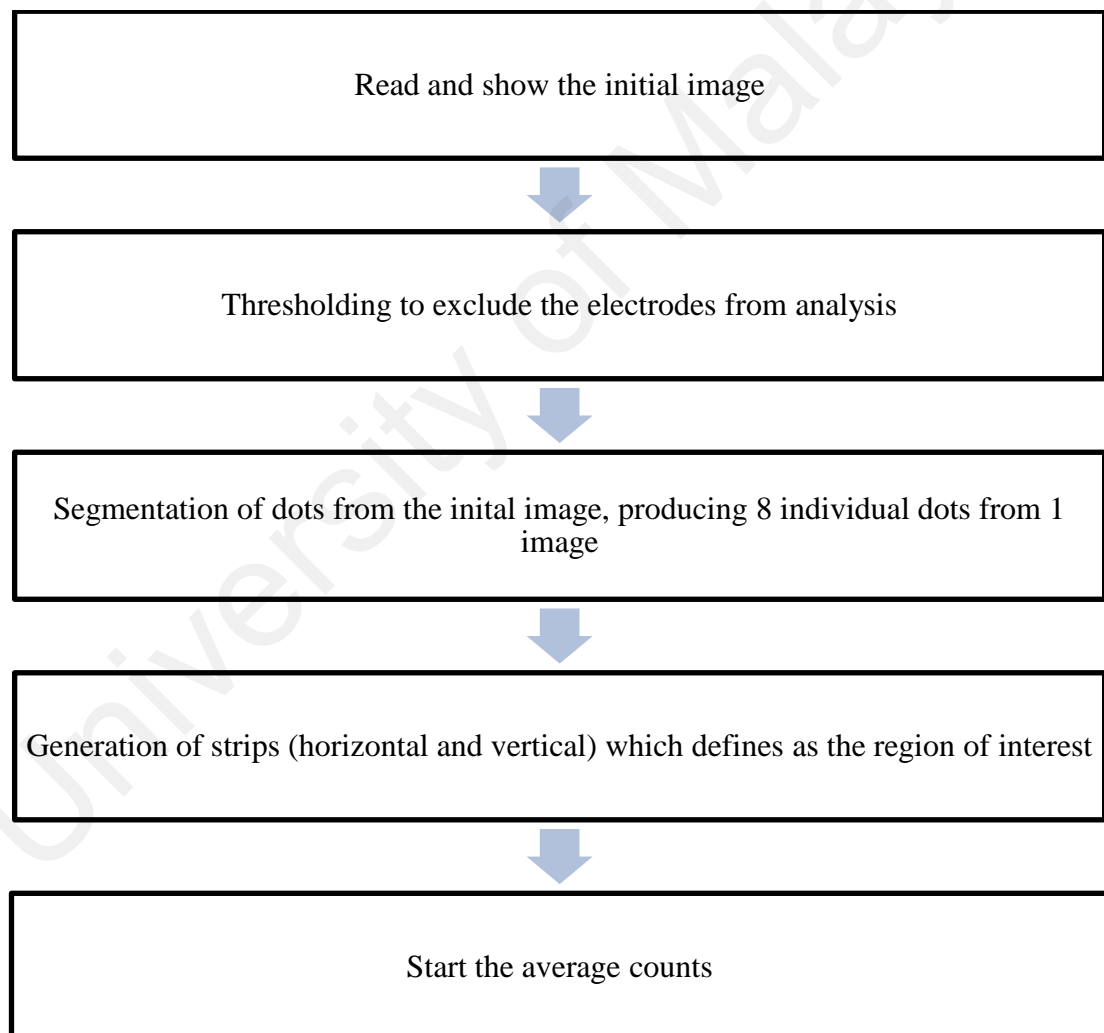


Figure 3.2: Flowchart of the whole process

3.2.1 Read and show original image

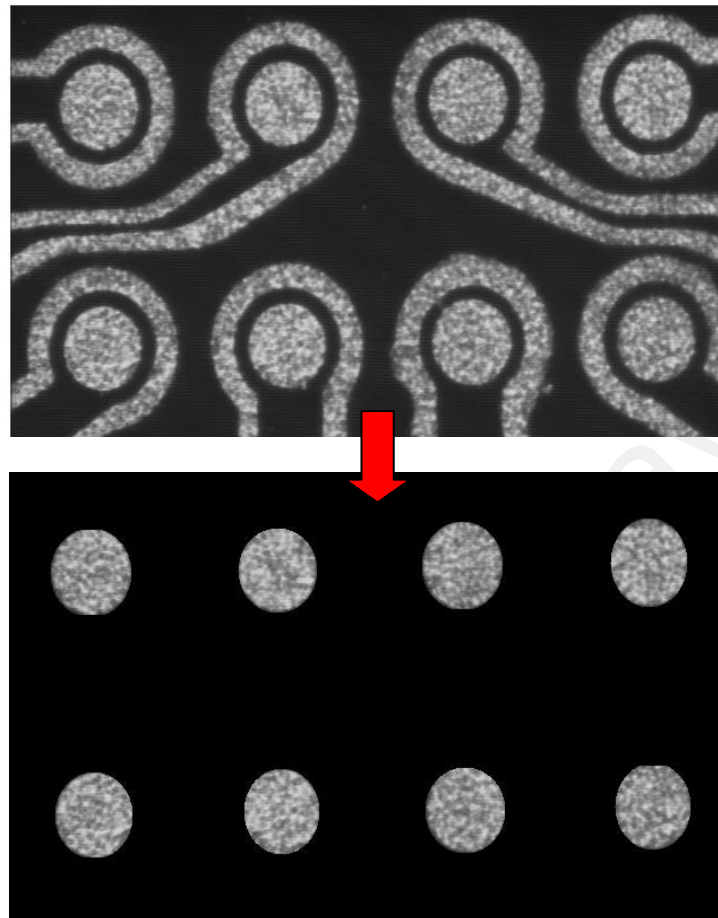


Figure 3.3: the process of elimination of non-profitable areas

Initially, the image was uploaded into the workspace and differentiation between electrodes and dots were completed before starting the analysis. This is done by finding and defining an area with a shape of a circle, thus eliminating the other areas by setting the grey level values to 0 which represents black. With this done, the electrodes will not come in the way in further processes of the image and no longer being an obstacle to be removed.

3.2.2 Segmentation of dots from the original image

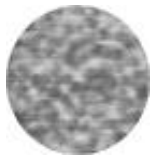
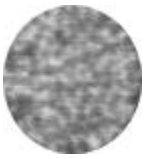
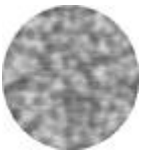
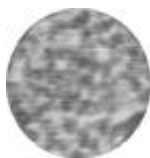
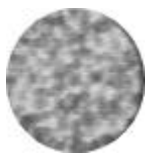
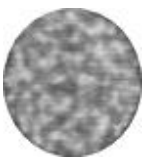
| | | | |
|---|---|--|---|
|  |  |  |  |
| 1 | 2 | 3 | 4 |
|  |  |  |  |
| 5 | 6 | 7 | 8 |

Table 3.1: Segmented dots from the original image

Each dot was extracted from an image, which will result in having 8 consecutive dots to be analyzed separately due to the fact that each dot will not have the same image intensity which was caused by the differences in the distribution of cells in each particular dot.

3.2.3 Generation of vertical and horizontal strips on each dots

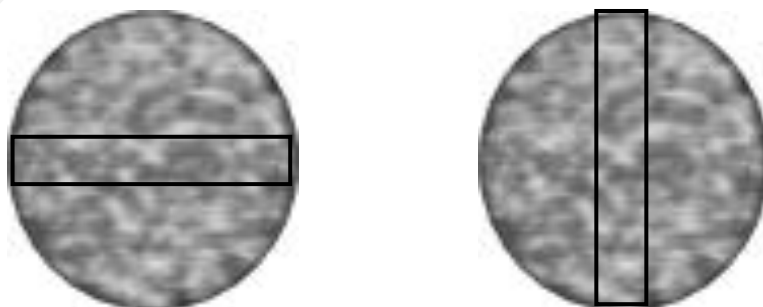


Figure 3.4: Development of horizontal and vertical strips

For each dot, 2 types of analysis will be conducted by using horizontal and vertical strips. The purpose of generating these strips is to define the region of interest for the analysis. The strips were generated by finding the start and end point in the first row of pixels values. This is done by determining the first point where the grey level value is less than 250, the threshold that was used in this analysis, and the end point is also determined by the same method. This can be further demonstrated by the figure below.

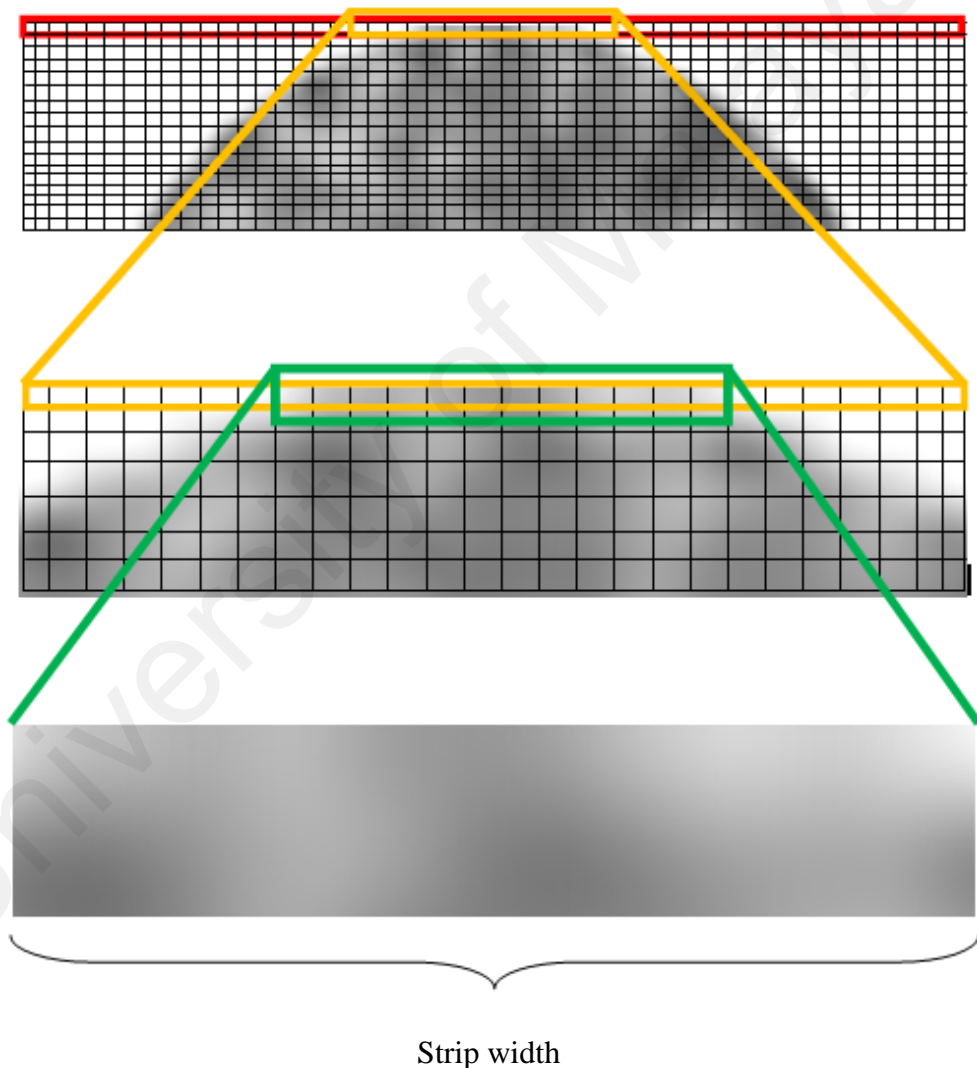


Figure 3.5: Magnified image of the process of dot extraction from an initial image

In the first row of pixel values on an image, there is an exact point where the boundary of a specific strip which will be defined as the start and end point of the strip. For example, in the figure above, the area in the red box is defined as the first row of pixel values for this image. From there, the start and end point of strip is where the pixel value is greater than 250.

3.2.4 From each strip, there are a few steps that have been done:

For the series of grey level values for each pixel, the average counts was applied by finding the mean of grey level values on 5 consecutive pixels and the value was stored temporarily in an array. Then, the averages of the next five pixels were found and so forth until the end of the row. These average values were then undergone statistical analysis where the standard deviation was found. From the standard deviation, it is predetermined that if a specified strip has average values with small range of standard deviation, the cell on the dot can be considered as evenly distributed.

In summary, the process of average counts technique starts with the segmentation process of dots from the original image. For a black and white image, the grey level was defined to be between 0 and 255 which represents the black and white respectively. From the dot images, the grey levels values of each pixel were recorded in an array which was then classified into segments with 5 pixels per segment. For each group of pixels (segment), the average value of grey levels was determined. A statistical analysis was conducted on the averages and standard deviation was determined. From the standard deviation, the values of maximum and minimum peaks will have to lie between 10 and 30 to be approved as images viable for experiments.

CHAPTER 4

RESULT AND DISCUSSION

To describe the results obtained from the analysis, there are a few factors that need to be clarified. Firstly, the segmentation of pixels. Throughout the image which consist of a large number of pixels (according to the image size), it is important that the pixels were grouped into an equal number of pixels. This is to maintain the stabilization of results obtained from the average counts.

The process of grouping pixels into segments is illustrated in the figure below. For each row, the pixels are taken 5 at a time and were numbered sequentially. From these pixel segments, then the average counts was done. From there, the results are shown in the table below. Secondly, the introduction of a standard deviation range between 10 and 30 on the plots assist the decision making process. Lastly, there are 2 sets of images used for this analysis which are evenly distributed cells are grouped as the first one and the unevenly distributed cells are grouped under the second set.

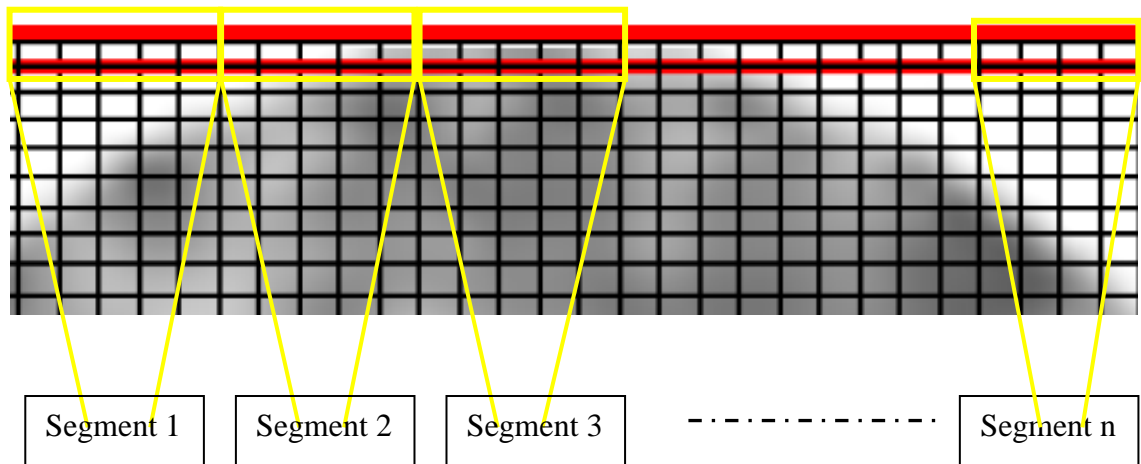
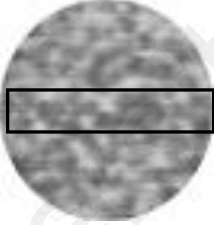
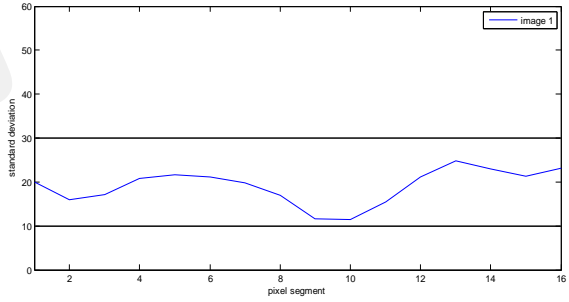
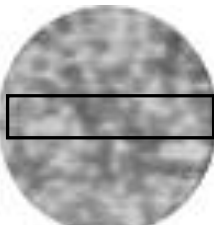
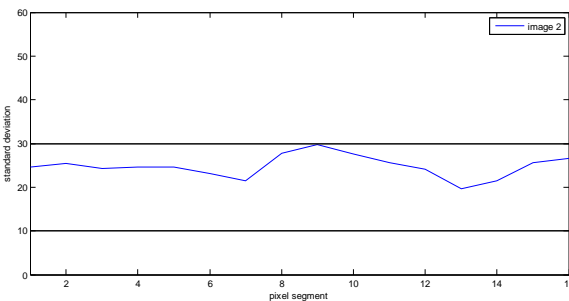
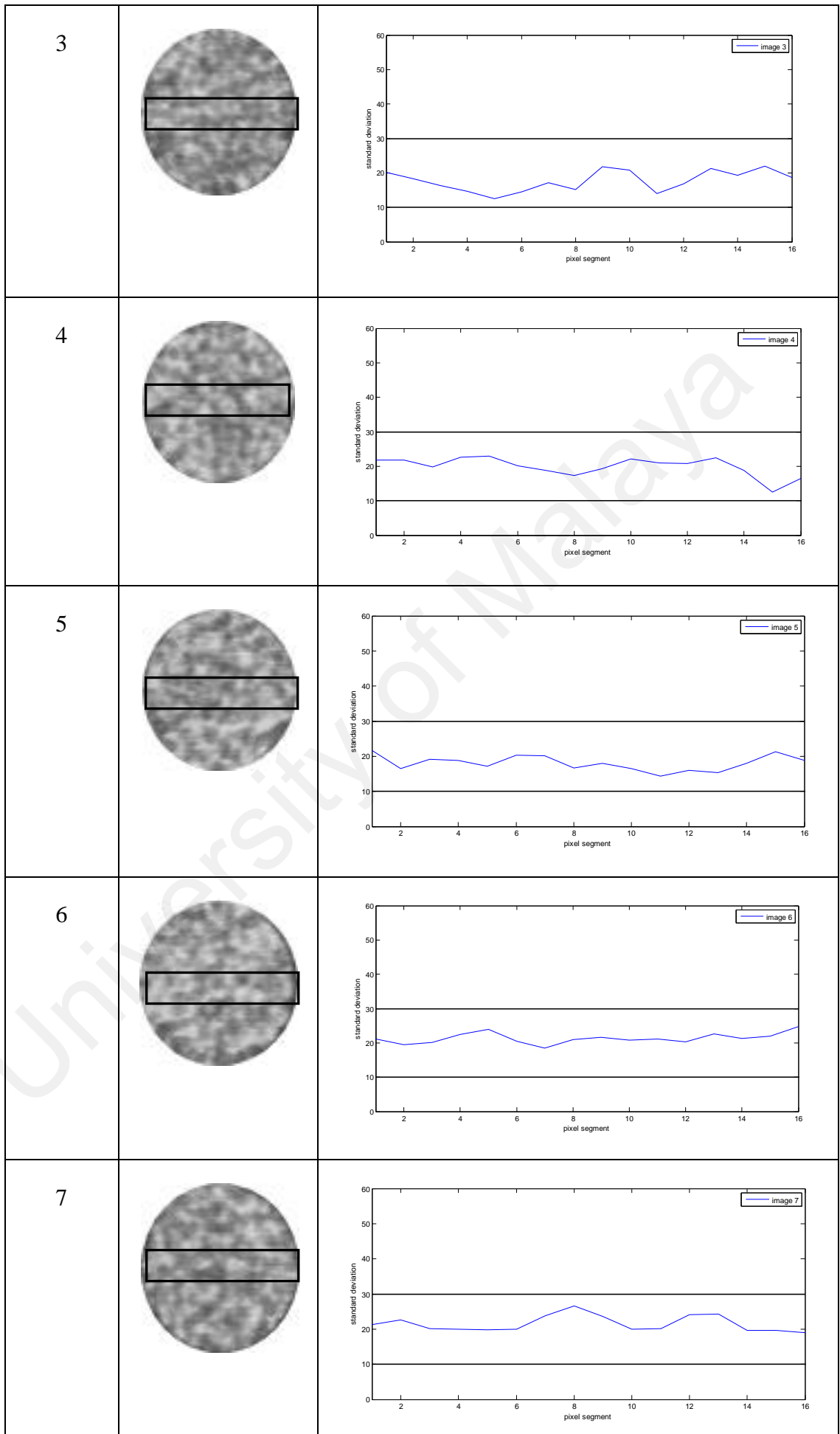


Figure 4.1: Classifying pixels into pixel segments

| Image number | Image for even distribution | Standard deviation plot of average counts (pixel segment vs. standard deviation) |
|--------------|---|--|
| 1 |  |  |
| 2 |  |  |



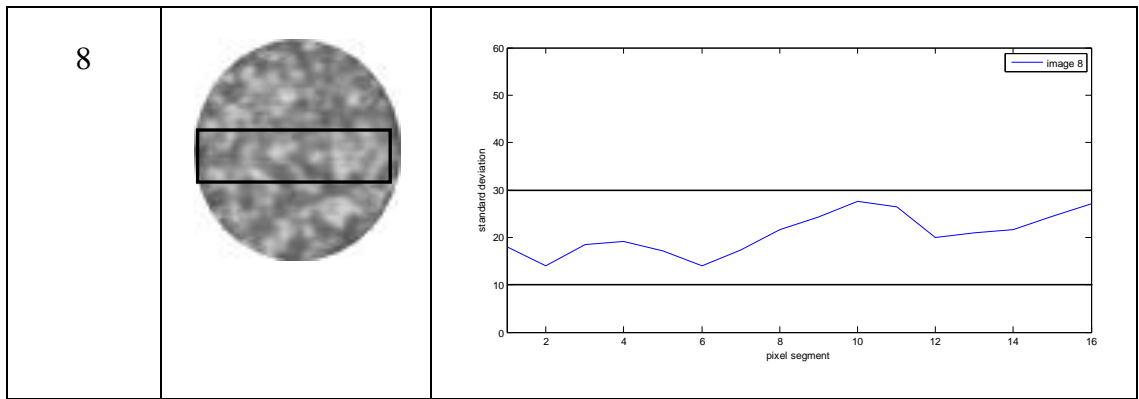
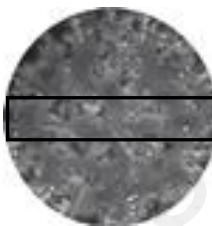
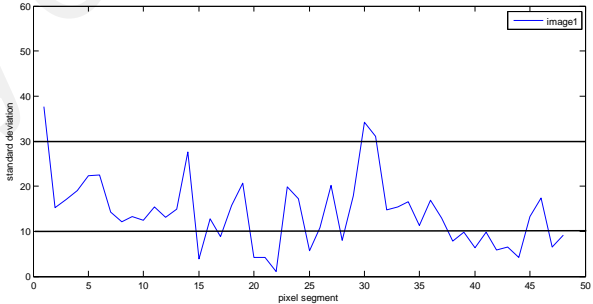
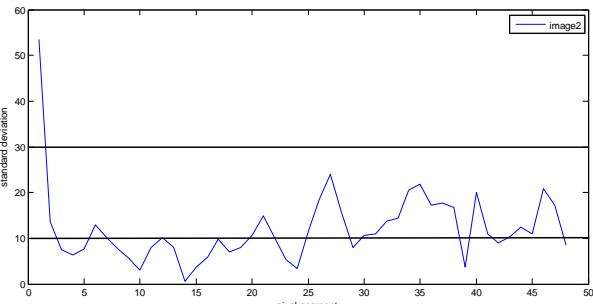
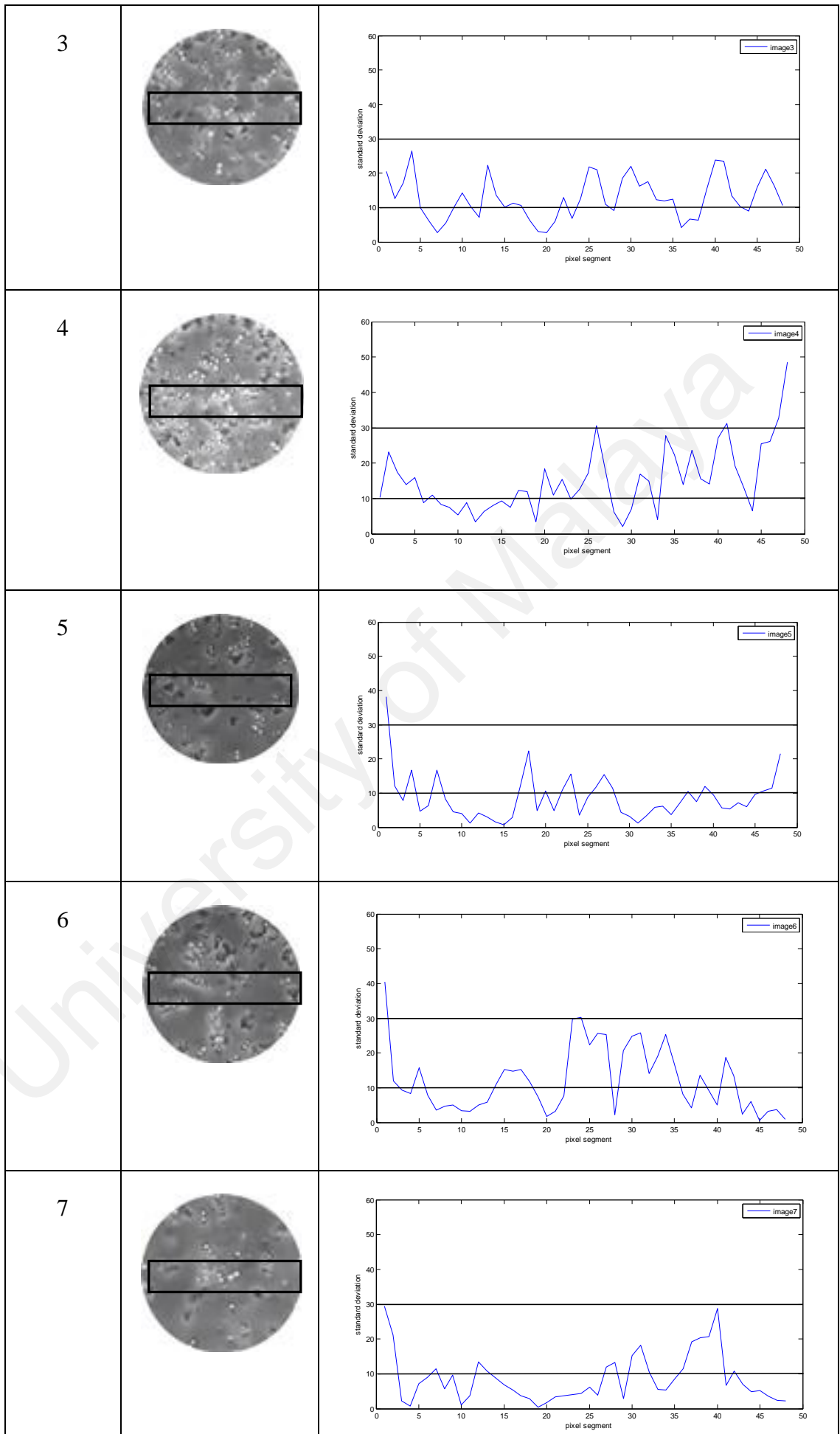


Table 4.1: pixel segment vs. standard deviation plot for images with even distribution of cells

| Image number | Image for uneven distribution | Standard deviation plot of average counts (pixel segment vs. standard deviation) |
|--------------|---|--|
| 1 |  |  |
| 2 |  |  |



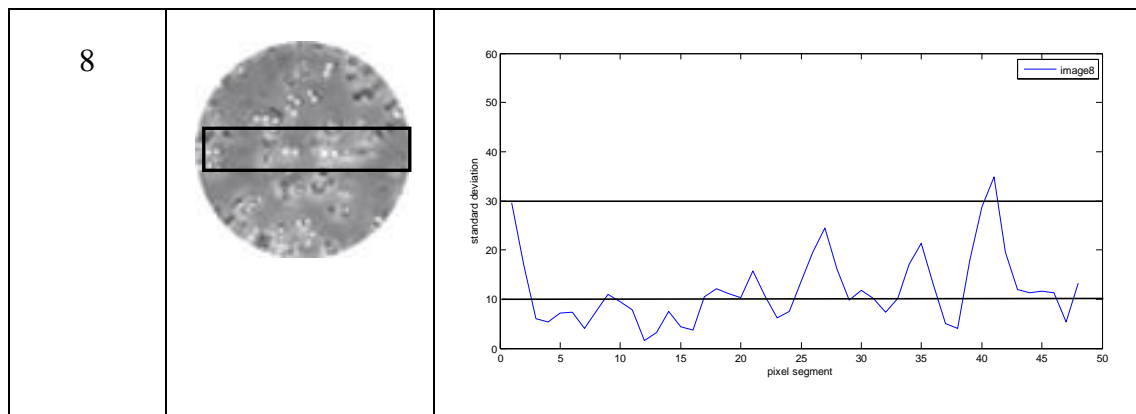


Table 4.2: pixel segment vs. standard deviation plot for images with uneven distribution of cells

Depicted in tables 4.1 and 4.2 are the results shown by horizontal strips taken from images of manually determined even and uneven distributions of cells. By introducing a boundary between 10 and 30, the standard deviation plots for the evenly distributed images are shown to lie in between the range. This is not so for the images of unevenly distribution of cells. As the plots in Table 2 illustrated, plots are randomly distributed with extreme values highly above and below the said boundaries.

In figure 4.2, the plots of the first set of data from the images of evenly distribution of cells, there exists no extreme value detected that lies above or beyond the boundary. This result contradicts from the other group of data which produces spikes and extreme values above and below the boundaries as depicted in figure 4.3. Thus, it is only fair to draw the conclusion that the said boundaries have the potential of determining the uniformity of cell distribution in a certain image.

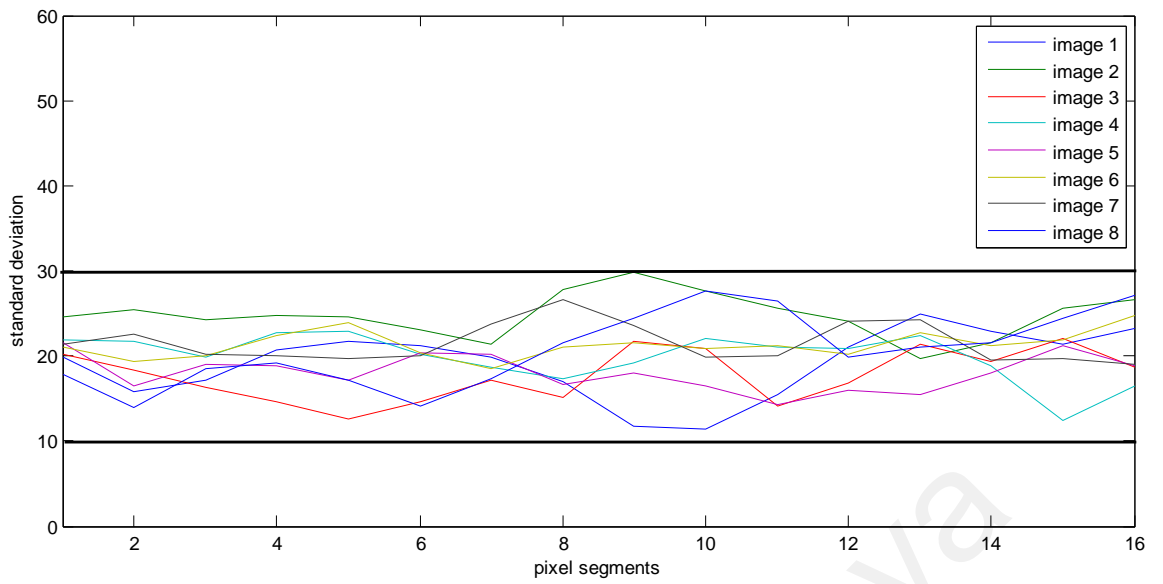


Figure 4.2: Standard deviation plots o the first group of images with evenly distributed cells

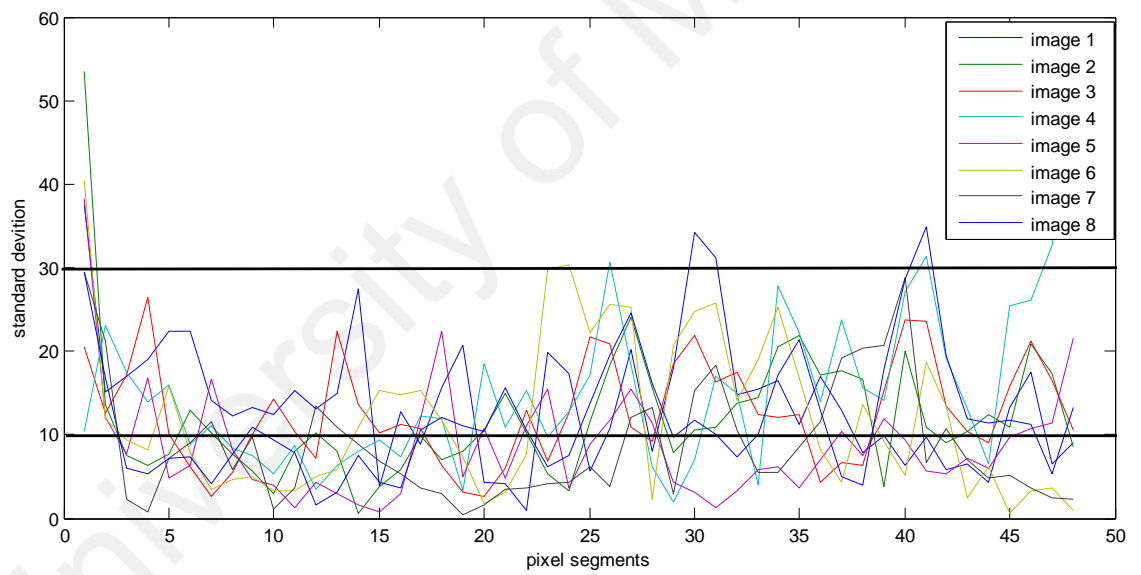


Figure 4.3: Standard deviation plots o the second group of images with unevenly distributed cells

CHAPTER 5

CONCLUSION

5.1 Summary

As promulgated previously in chapter 1, all DEP experiments must be inserted with a gasket full of cells which are being distributed evenly throughout the dot area. Previously, the initiation of DEP experiments were only using single dot electrodes which eliminate the needs of image analysis prior starting an experiment. This is because the algorithm developed by Fatoyinbo *et al.* (2008) for single dot experiments are proven to be effective and impeccably resonable. Unfortunately, recent advancement on electrode development which have moved from single to multiple dot electrodes denies the immunity of the previous algorithm. Thus average counts is adapted to meet this purpose. The findings from the average count algorithm implies that standard deviation can be used to evaluate the effectiveness of the said algorithm. The introduction of a range between 10 and 30 makes the process of analyzing the data to be much more yielding. It is prominent to say that images with even distribution of cells will produce a standard deviation plot that lies within the boundaries of 10 and 30.

5.2 Limitation

There are a few limitations of this method since it is not fully tested and applied. Firstly, this method is fully dependent on the contrast and brightness of the original image provided from previous experiments with the contrast and brightness of the images differ from one to another. Secondly, there are only limited number of images undergone this algorithm to fully concluded that the results provided are representative of the whole images. Other than that, there are limited resources and time constrain faced for this short dissertation.

5.3 Future Recommendations

For future work, there are a few recommendations that can be adopted in order to improve the current work. Most importantly, the analysis of graph produced from the standard deviation plots must be extended by applying Fourier Transform. This is to determine the homogeneity and uniformity of the cell distribution from an optical based DEP devices by giving out a numerical value. Besides that, the currently developed algorithm can be incorporated into the overall DEP analysis program that have been developed previously by Kadri (2010).

REFERENCES

- Becker, F. F., Wang, X. B., Huang, Y., Pethig, R., Vykoukal, J., & Gascoyne, P. R. C. (1994). The Removal of Human Leukemia-Cells from Blood Using Interdigitated Microelectrodes. *Journal of Physics D-Applied Physics*, 27(12), 2659-2662.
- Becker, F. F., Wang, X. B., Huang, Y., Pethig, R., Vykoukal, J., & Gascoyne, P. R. C. (1995). Separation of Human Breast-Cancer Cells from Blood by Differential Dielectric Affinity. *Proceedings of the National Academy of Sciences of the United States of America*, 92(3), 860-864.
- Broche, L. B., N.; Lewis, M.; Porter, S.; Hughes, M. & Labeed, F. . (2007). Early detection of oral cancer-Is dielectrophoresis the answer? *Oral oncology* 43(2), 199–203.
- Broche, L. L., F. & Hughes, M. . (2005). Extraction of dielectric properties of multiple populations. *Physics in Medicine and Biology* 50, 2267–2274.
- Chin, S., Hughes, M. P., Coley, H. M., & Labeed, F. H. (2006). Rapid assessment of early biophysical changes in K562 cells during apoptosis determined using dielectrophoresis. *International Journal of Nanomedicine*, 1(3), 333-337.
- Crane, J. P., H. . (1968). A study of living and dead yeast cells using dielectrophoresis. *Journal of the Electrochemical Society*, 115, 584.
- Fatoyinbo, H. O., Hoettges, K. F., & Hughes, M. P. (2008). Rapid-on-chip determination of dielectric properties of biological cells using imaging techniques in a dielectrophoresis dot microsystem. *Electrophoresis*, 29(1), 3-10.
- Fatoyinbo, H. O., Kadri, N. A., Gould, D. H., Hoettges, K. F., & Labeed, F. H. (2011). Real-time cell electrophysiology using a multi-channel dielectrophoretic-dot microelectrode array. *Electrophoresis*, 32(18), 2541-2549.
- Gascoyne, P. R. C., Huang, Y., Pethig, R., Vykoukal, J., & Becker, F. F. (1992). Dielectrophoretic Separation of Mammalian-Cells Studied by Computerized Image-Analysis. *Measurement Science & Technology*, 3(5), 439-445.
- Gascoyne, P. R. C., & Vykoukal, J. (2002). Particle separation by dielectrophoresis. *Electrophoresis*, 23(13), 1973-1983.
- Hoettges, K. F., Hubner, Y., Broche, L. M., Ogin, S. L., Kass, G. E. N., & Hughes, M. P. (2008). Dielectrophoresis-activated multiwell plate for label-free high-throughput drug assessment. *Analytical Chemistry*, 80(6), 2063-2068.
- Huang, Y. W., X.; Becker, F. & Gascoyne, P. . (1996). Membrane changes associated with the temperature-sensitive P85gag-mos-dependent transformation of rat kidney cells as determined by dielectrophoresis and electrorotation. *Biochimica et Biophysica Acta (BBA)-Biomembranes* 1282(1), 76–84.
- Hubner, Y., Mulhall, H., Hoettges, K. F., Kass, G. E. N., Ogin, S. L., & Hughes, M. P. (2007). Dielectrophoresis: A new in vitro approach to measure drug-induced cytotoxicity. *Toxicology*, 240(3), 183-184.
- Hughes, M. P. (2002). Strategies for dielectrophoretic separation in laboratory-on-a-chip systems. *Electrophoresis*, 23(16), 2569-2582.
- Jones, K. S., J. . (1985). An improved method to determine cell viability by simultaneous staining with fluorescein diacetate-propidium iodide. *Journal of histochemistry and cytochemistry*, 33(1), 77.

- Jones, T. B. (1995). Electrical forces and torques on bioparticles. *Electrostatics 1995*, 143, 135-144.
- Jones, T. B. (2003). Basic theory of dielectrophoresis and electrorotation. *Ieee Engineering in Medicine and Biology Magazine*, 22(6), 33-42.
- Jones, T. B., Fowler, J. D., Chang, Y. S., & Kim, C. J. (2003). Frequency-based relationship of electrowetting and dielectrophoretic liquid microactuation. *Langmuir*, 19(18), 7646-7651.
- Labeed, F. C., H.; Thomas, H. & Hughes, M. (2003). Assessment of multidrug resistance reversal using dielectrophoresis and flow cytometry. *Biophysical journal* 85(3), 2028–2034.
- Labeed, F. H., Coley, H. M., & Hughes, M. P. (2006). Differences in the biophysical properties of membrane and cytoplasm of apoptotic cells revealed using dielectrophoresis. *Biochimica Et Biophysica Acta-General Subjects*, 1760(6), 922-929.
- Labeed, F. H., Coley, H. M., Thomas, H., & Hughes, M. P. (2003). Assessment of multidrug resistance reversal using dielectrophoresis and flow cytometry. *Biophysical Journal*, 85(3), 2028-2034.
- Lee, R. S., Arnold, W. M., & Pethig, R. (2004). Control of cell elution from a dielectrophoresis micro-array using a permittivity gradient. *2004 Annual Report Conference on Electrical Insulation and Dielectric Phenomena*, 352-355.
- Pethig, R. (2010). Review Article-Dielectrophoresis: Status of the theory, technology, and applications. *Biomicrofluidics*, 4(2).
- Pethig, R., & Markx, G. H. (1997). Applications of dielectrophoresis in biotechnology. *Trends in Biotechnology*, 15(10), 426-432.
- Pohl, H. A. (1951). Dielectrophoresis. *J of Applied Physics*(22), 869.
- Pohl, H. H., I. (1966). Separation of Living and Dead Cells by Dielectrophoresis. *Science (New York, NY)* (152(3722)), 647.
- Pohl, H. K., K. & Pollock, K. (1981). The continuous positive and negative dielectrophoresis of microorganisms. *Journal of Biological Physics* 9(2)(67–86).
- Wang, X. H., Y.; Gascoyne, P.; Becker, F.; Hölzel, R. & Pethig, R. (1994). Changes in Friend murine erythroleukaemia cell membranes during induced differentiation determined by electrorotation. *Biochimica et biophysica acta* 1193(2), 330.
- Wang, X. J., Becker, F. F., & Gascoyne, P. R. C. (2002). Membrane dielectric changes indicate induced apoptosis in HL-60 cells more sensitively than surface phosphatidylserine expression or DNA fragmentation. *Biochimica Et Biophysica Acta-Biomembranes*, 1564(2), 412-420.
- Yang, J. H., Y.; Wang, X.; Wang, X.; Becker, F. & Gascoyne, P. . (1999). Dielectric properties of human leukocyte subpopulations determined by electrorotation as a cell separation criterion. *Biophysical journal* 76(6), 3307–3314.
- Kadri, N. A. (2010). Development of near real-time assessment system for cancer cells. *University of Surrey, Surrey GU2 7TE*.

APPENDIX A

MATLAB codes for average counts

```
function [ V ] = av5( I,v )

M=size(I,1);    %bace satu row and define the length of row(bilangan
column)

for i=1:M
    V(i,:)=rav5(i,I,v); %cari average in a row, 5 by 5
end

function [VR]=rav5(i,I,v)

N=size(I,2);
n=mod(N,v);
R=(N-n)/v;

for j=1:R
    VR(j,1)=avrr(i,j,I,v);    %for nilai yg cukup2 dlm gandaan v
end

if n>0
    VR(R+1,1)=avrn(i,n,R*v,I);    %for nilai yg balance, luar dr gandaan
    v
end

function [VRJ]=avrr(i,j,I,v)

P=I(i,(v*(j-1)+1):v*j);
VRJ=sum(P)/v;

function [VRR]=avrn(i,n,Rv,I)

P=I(i,Rv+1:Rv+n);
VRR=sum(P)/n;
```